CHANGES IN THE FLOW STRUCTURE AND ENERGY LOSS OF A TSUNAMI CURRENT THROUGH FOREST WITH A GAP

NAVEED ANJUM
Graduate School of Science and Engineering, Saitama University, Saitama, Japan, shayank33@gmail.com

NORIO TANAKA
Graduate School of Science and Engineering, Saitama University, Saitama, Japan, tanaka01@mail.saitama-u.ac.jp

International Institute for Resilient Society, Saitama University, Saitama, Japan

ABSTRACT

The disastrous events of tsunamis or floods in the past revealed the effectiveness of coastal forest. In tsunami mitigation strategies, interest in a multiple defense system is increasing rather than a single defense structure. This shift to a multiple defense system because the tsunami inundation could sufficiently be delayed and the overflow volume could be reduced compared to that of a single defense system. The previous research studies pointed out the limitation of land use in the coastal area, which is a major problem to construct a thick forest for tsunami mitigation. Thus, the present study conducted flume experiments to clarify the flow structure and energy loss through a forest with a gap, i.e. discontinuous forest model (DFM), under varying steady subcritical flows and varying gaps between the forest models. An experiment with continuous forest model (CFM) was also performed under the same flow conditions for the comparison purpose. The discontinuous forest, i.e. combination of upstream model (UM) and downstream model (DM), resulted in slightly larger backwater rise, i.e. 1-6%, upstream of the models due to higher flow resistance, as compared to that of continuous forest. Hence, due to double reflection (back movement of water wave due to backwater rise) and large resistance offered by DFM, the maximum loss of flow energy became higher, i.e. 37%, compared to that of CFM, i.e. 32%. The results demonstrate that this type of discontinuous forest with the appropriate configuration could be as effective as a continuous forest belt in mitigating the tsunami hazards.

Keywords: Tsunami, coastal forest, disaster reduction, flow structure, energy loss

1. INTRODUCTION

The 2011 Great East Japan tsunami (GEJT) caused great damage to the hard structures like sea walls, tsunami gates, and large embankments (Tappin et al., 2012) as well as coastal forests (Tanaka et al., 2013). It hence destroyed people lives and buildings in the Tohoku and Kanto regions of Japan (Suppasri et al., 2013). However, the previous tsunami events like 1998 Papua New Guinea tsunami (Dengler and Preuss, 2003), 2004 Indian Ocean tsunami (Tanaka et al., 2007), and 2011 GEJT (Nandasena et al., 2012) also revealed the effectiveness of natural defense system like a coastal forest. The coastal forest plays a significant role in providing resistance to the tsunami flow and floods by narrowing the passage of fluid flow; and thus, resulting in the reduction of fluid force as well as the energy of the flow (Harada and Imamura, 2006; Tanaka et al., 2014). Contrarily, the limitation of a coastal forest for tsunami mitigation has also been discussed concerning the destruction of the coastal forest itself (Tanaka et al., 2007) and the production of driftwood (Dengler and Preuss, 2003). However, the previous studies (Tanaka, 2012; Pasha and Tanaka, 2016) pointed out that even after the large destruction of the coastal forest, it still acts to mitigate the tsunami damage by capturing tsunami borne floating debris. Therefore, an inland forest as a secondary defense system was proposed by previous researchers (Tanaka et al., 2013; Anjum and Tanaka, 2019) that could become a stronger shield against approaching tsunamis as well as capturing driftwood.

For mitigating the damage due to tsunamis, the approach has been changed from single to compound defense system (Igarashi and Tanaka, 2018). Recently, the number of studies that propose compound defense systems, i.e., forest with a moat (Usman et al., 2014), double embankment system (Tanaka and Igarashi, 2016), and hybrid defense system comprising of an embankment with coastal forest (Tanaka et al., 2014; Rashedunnabi and Tanaka, 2019), has drawn much attention. The limitation of land use in the coastal area is a major obstacle to construct a thick forest for tsunami mitigation. Yang et al. (2017) also pointed out that patch type vegetation with a certain size, rather than a continuous vegetation belt, may be sufficient for mitigating tsunami damage. However, no study has been reported yet elucidating the comparison of a continuous and discontinuous forest

of the same thickness and the forest configuration. In addition to this, the gap between the discontinuous forest is a very important parameter that could play an effective role, focused on maximum energy reduction and minimum land utilization. Thus, there is a need to develop an effective and reasonable solution in order to strengthen the natural defense system against the tsunami inundation.

Therefore, the present experimental study investigated whether the discontinuous forest could provide sufficient resistance and energy reduction in comparison to that of a continuous forest. The effectiveness of varying gap length between the discontinuous forest models was also investigated in this study. This study focused on flow structure and energy loss of the inland-approaching-tsunami current.

2. MATERIALS AND METHODS

2.1 Experimental setup and flow conditions

The experiments were performed in a laboratory flume (dimensions: 14m × 0.5m × 0.7m) with a constant bed slope of 1/700 at Saitama University, Japan (Figure 1a), where the tsunami characteristics were considered generally and were not specific to any location. The discharge in the flume was controlled with the help of a flow-controlling PC using a measurement software program (HYDRA). An inundating tsunami flow was observed to be subcritical (Froude number between 0.6 and 1) (Spiske et al., 2010; Tanaka et al., 2013; Tanaka et al., 2014). Therefore, to set the flow conditions in the present study, Froude similarity was applied for setting the model scale of the physical experiment. The initial Froude number (Fr_o) with reference to the initial water depth and initial flow velocity was used without a forest model. For achieving subcritical flow conditions of an inundating tsunami current, the initial water depths "h_o" (without forest model) in the flume were considered as 3.5, 4.5, 5.8, 7.3, 8.6, and 9.3cm, which gave Fr_o approximately equal to 0.650, 0.677, 0.696, 0.702, 0.712, and 0.721, respectively. Thus, a similar range of Froude values as that of the actual tsunami inundation was adopted in this study. Moreover, as mentioned in the previous studies (Tanaka et al., 2013; Pasha and Tanaka, 2016), it is suitable to construct a coastal forest inland, where it can capture tsunami-borne floating debris. From that perspective, the flow condition is set in the lower range of Froude numbers in the post-tsunami investigation (Spiske et al., 2010; Tanaka et al., 2014).

2.2 Model design and measurement

A physical scale of 1/100 was selected for the experimental models. In the Indian Ocean tsunami, trees with a diameter greater than 0.3m along the coastline of some regions in Sri Lanka were not damaged, and those trees with a large trunk diameter were also noticed to be sparse (Tanaka et al., 2007). Moreover, referring to the Japanese pine tree (average tree trunk diameter= 0.4m) found on the Sendai Plain (Tanaka, 2012), the wooden circular cylinder of 0.4cm diameter (considering 1/100 model scale) was used as a tall tree model. Following the previous research works (Pasha and Tanaka, 2017; Rashedunnabi and Tanaka, 2019), the crown part of the tree was not considered in the physical modeling of this experiment for simplicity, and hence, mainly the trunk part was modeled. The cylinders were mounted on a flat plate (as shown in Figure 1a) in a staggered arrangement for the construction of sparse (G/d= 2.125, where G is the clear spacing between the cylinders and d is the diameter of the cylinder) emergent forest models. The forest models covered the full width of the flume while maintaining a small gap between the outer cylinder (the cylinder at the cross-wise boundary of the modeled forest) and the flume wall. The ratio between the flume width and the cylinder diameter should be greater than 5 in order to minimize sidewall effects on the flow structure (Rashedunnabi and Tanaka, 2019). Hence, this ratio was maintained to minimize the sidewall effects in the present study. The forest model was placed on the flume bed at a distance of approximately 3m from the channel inlet. The forest arrangement details are given in Figure 1b and Table 1.

Initially, a continuous forest model with a longitudinal width of "W" (the scheme of which is shown in Figure 1c) was tested for comparison purpose. The discontinued forest models (with each having half longitudinal width "$W/2$") were also tested in the flume with varying gap condition between the upstream and downstream forest models, i.e. Gap= 8, 6, 4, and 0.5m, in order to clarify the effectiveness of gap between the forests (Figure 1d). The forest width (in the direction of flow) and center to center distance between trees (D= 2.5cm) were considered with respect to the forest thickness "dn" ($=2Wd/(\sqrt{3}D^2) \times 10^2$) (Pasha and Tanaka, 2017). In this study, the density of trees in the forest is represented in terms of G/d and porosity ($P_r = 1\text{-}n_t d2\pi/4$, where n_t denotes the number of trees per unit area) (Iimura and Tanaka, 2012).

The flow depth was measured along the centerline of the flume channel with the help of a rail-mounted point gauge. Measurements were taken at small intervals, along the flume channel, depending on the variation in water surface. The depth-averaged velocity (V) was calculated using the measured water depth and known discharge with the help of continuity equation $Q= AV$, where Q is the discharge and A is the cross-sectional area.

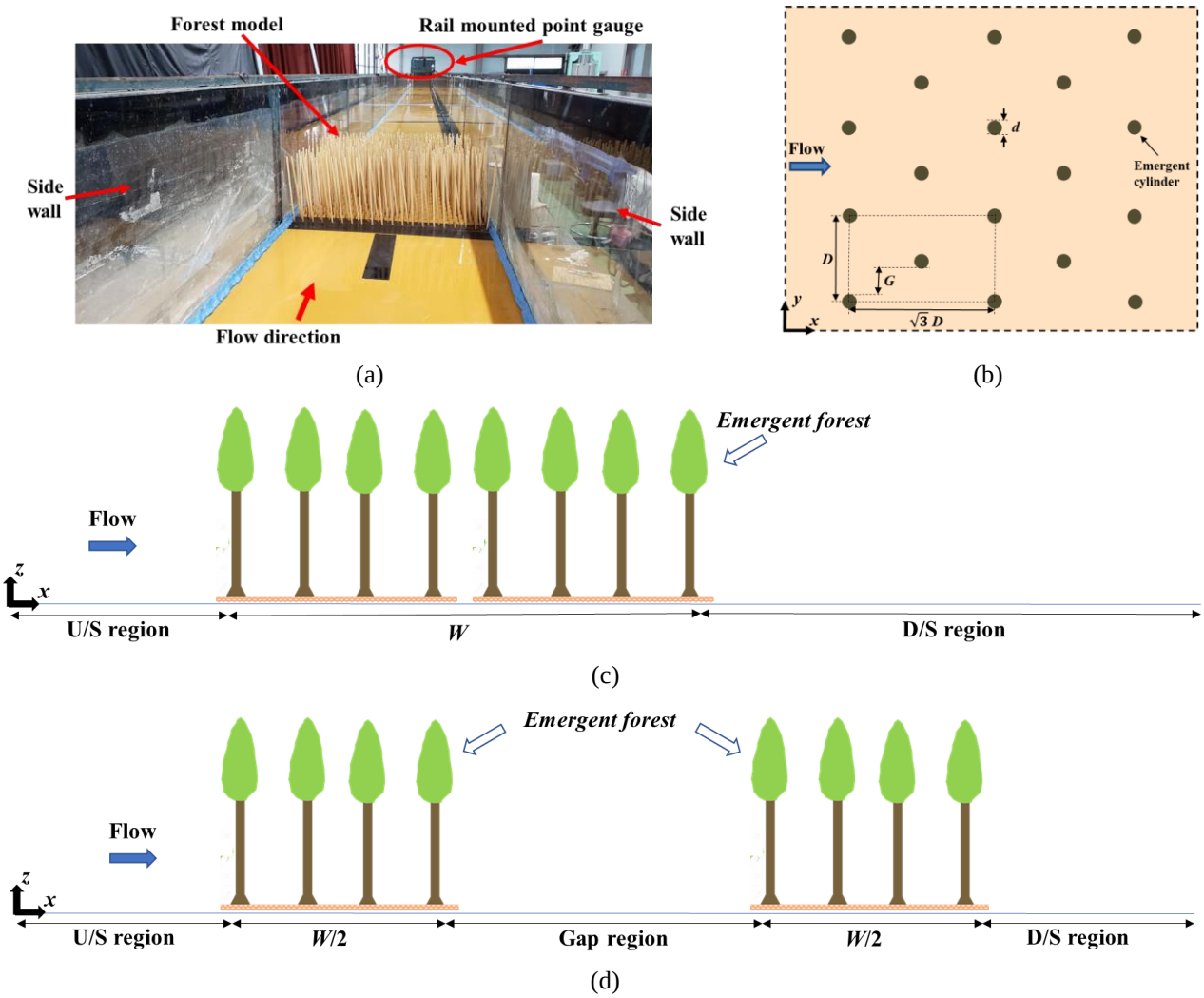

Figure 1: Experimental setup: (a) experimental flume with forest model, (b) plan view scheme of emergent cylinder arrangement, (c) scheme for side view of continuous forest model, and (d) scheme for side view of discontinuous forest model, i.e. forest model with a gap.

Table 1. Vegetation configuration and experimental conditions, where UM and DM represent the upstream model and downstream model, respectively, W is the width of the forest, dn is the vegetation thickness, P_r is the porosity of forest, and Fr_o is the initial Froude number.

	CONFIGURATION	GAP (m)	FOREST TYPE	W (cm)	dn (No. cm)	P_r (%)	Fr_o
1	Continuous Forest	n/a	Sparse (Tall)	48.54	358.72	98	0.650,0.677, 0.696, 0.702, 0.712, 0.721
2	Discontinuous Forest	8, 6, 4, 0.5	UM-Sparse (Tall) DM-Sparse (Tall)	24.27 24.27	179.36 179.36	98 98	0.650,0.677, 0.696, 0.702, 0.712, 0.721

3. RESULTS AND DISCUSSION

3.1 Flow structure around forest models

After the placement of forest models in the experimental flume, the flow structures through these structures significantly varied with the change in flow as well as forest conditions. Figure 2 shows the resulting water surface profile against the maximum Fr_o condition for all the considered configurations and gaps between the forests. The water depth without forest models, critical depth, and resulting flow structure classification are also displayed in Figure 2. It is clearly visible that the flow (which was almost uniform without forest models) experienced noteworthy variations in the upstream of forest models, within the forest region, as well as in the downstream region due to the resistance offered by the staggered arranged cylinders. These variations around the forest models became more significant with the increase in Fr_o condition. Due to the drag offered by the forest in all the considered configurations, a rise in the flow depth in the upstream of forest models was found as compared to that of initial water depth. The presence of trees in the forest models narrowed the passage of fluid flow, the resistance of which created a difference in water level in the upstream and downstream of forests; thus, resulted in a water surface slope inside the models. In addition to this, the flow depth in the

downstream region was also observed to be significantly reduced, followed by large undulations. A clear difference in the water surface profiles can be observed between the continuous forest model (CFM) and discontinuous forest models (DFMs). The detailed flow structures are explained in the following subsections:

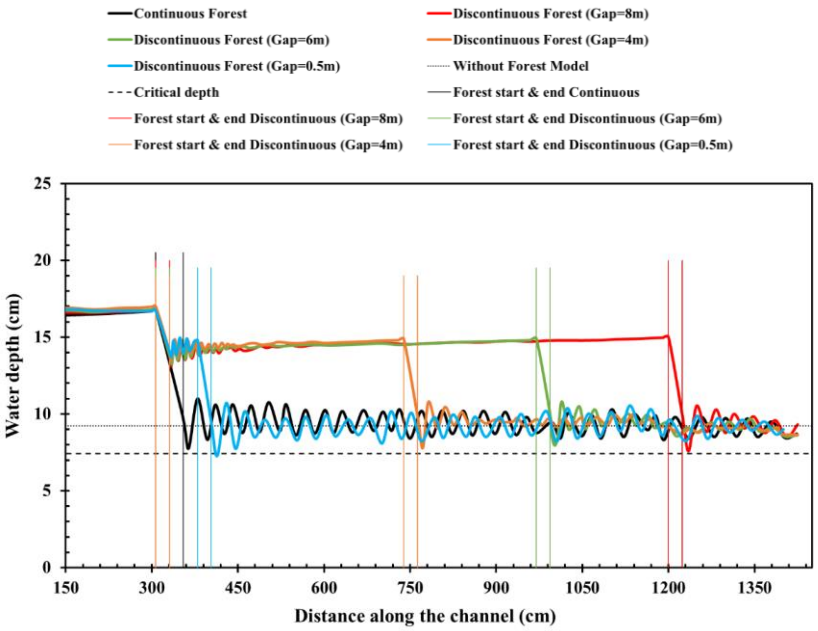

Figure 2: Water surface profiles for all the cases against the highest initial Froude number condition, i.e. Fr_o= 0.721.

3.1.1Backwater rise

The backwater rise ($\Delta h = h - h_o$, where h is the water rise in the upstream of forest model and h_o is the initial water depth) in the upstream region of the forest for all the cases is presented in Figure 3(a). The backwater rise showed a noteworthy rising trend with the increase in Fr_o condition for all the considered configurations. It can be observed that the backwater rise is slightly higher, i.e. approximately 1-6%, for DFM cases in comparison to that of CFM case, despite the fact that the forest thickness for both configurations, i.e. CFM and DFM, is same. This is due to the reason of double reflection offered by the double defense system in DFM configuration, indicating an advantage of discontinued forest over the continued forest in providing resistance to the approaching tsunami current. Contrarily, the difference in the backwater rise for DFM cases is not clearly observed with the variation in the gap region between the forest models. However, slightly higher magnitudes in backwater rise are observed for the DFMs with lower gap regions, i.e. Gap= 4m and 0.5m, as compared to those of comparatively higher gap regions, i.e. Gap= 8m and 6m, which might be due to the slightly stronger reflection effect of the DMs on the backwater rise. Moreover, the backwater rise for the UMs was also observed to be significantly higher in comparison to that of the backwater rise for the DMs.

3.1.2Water surface slope

Figure 3(b) shows the water surface slope "$tan\ \theta$" within the forest models for all the cases. The higher difference in the water level between the upstream and downstream regions of the forest models due to large resistance results in higher water surface slope inside the forest region (Pasha and Tanaka, 2017). A gradually rising trend in water surface slope is found with the increment in Fr_o condition. A clear difference in water surface slope between the CFM case and DFM cases can be seen. The slope magnitudes became slightly higher for CFM case in comparison to those of DFM cases of UMs, which is due to the reason that the DMs in DFM configurations raised the flow depth in their upstream regions. This resulted in lower difference in water levels between the upstream and downstream regions of UMs; and hence, consequently resulted in relatively lower magnitudes of water surface slopes. It demonstrates that the flow structure around the UMs is affected by the influence of the DMs, showing consistency with the results found by Anjum and Tanaka (2019). Furthermore, the slope magnitudes for the UM in DFM case with minimum gap condition i.e. Gap= 0.5m, are also found to be low. This is due to the reason of higher reflection effect of the DM as well as the continued undulations in the gap between the forest models (as can be easily seen in Figure 2). On the other hand, the magnitudes of slopes are found to be significantly higher for DMs in all the DFM cases in comparison to that of CFM. This result of higher water surface slopes inside the DMs is reasonable because of a comparatively higher ratio of raised flow depth in their upstream region to the forest width in the flow direction. Moreover,

the DM for minimum gap case, i.e. Gap= 0.5m, experienced noticeably higher magnitudes of slopes among all the cases, which is due to the reason of larger difference of flow depth in its upstream and downstream regions.

3.1.3Downstream inundation depth

Contrary to the rise in flow depth upstream of the forest model, the resistance offered by the forest results in the reduction of inundation depth downstream of it (Harada and Imamura, 2005; Iimura and Tanaka, 2012). The non-dimensional inundation depth (*h'*) in the downstream region of the forest model for all the cases against the considered Fr_o conditions is presented in Figure 3(c). The inundation depth (h_i) is normalized with respect to the initial water depth (h_o). Despite the fact that the data shows a slightly decreasing trend in *h'* with the increase in Fr_o condition, the downstream inundation depth is not significantly affected due to varying forest arrangement. For the lower range of Fr_o condition, i.e. Fr_o= 0.650,0.677, and 0.696, the *h'* became slightly higher for DFM cases with Gap= 8, 6, and 4m; however, the reduction in the downstream flow depth appear almost similar for all the CFM and DFMs cases against a higher range of Fr_o condition, i.e. Fr_o= 0.702, 0.712, and 0.721. Contrarily, the DFM case with minimum considered gap, i.e. Gap= 0.5m, between the forest models showed slightly lower magnitudes of *h'* in comparison to those of other DFM cases as well as CFM case against all the considered Fr_o conditions. Thus, the stronger reflection effect (followed by continued undulations in the gap region as shown in Figure 2) of DM with minimum gap condition significantly influenced not only the backwater rise in the upstream region but also slightly influenced the flow depth in the downstream region.

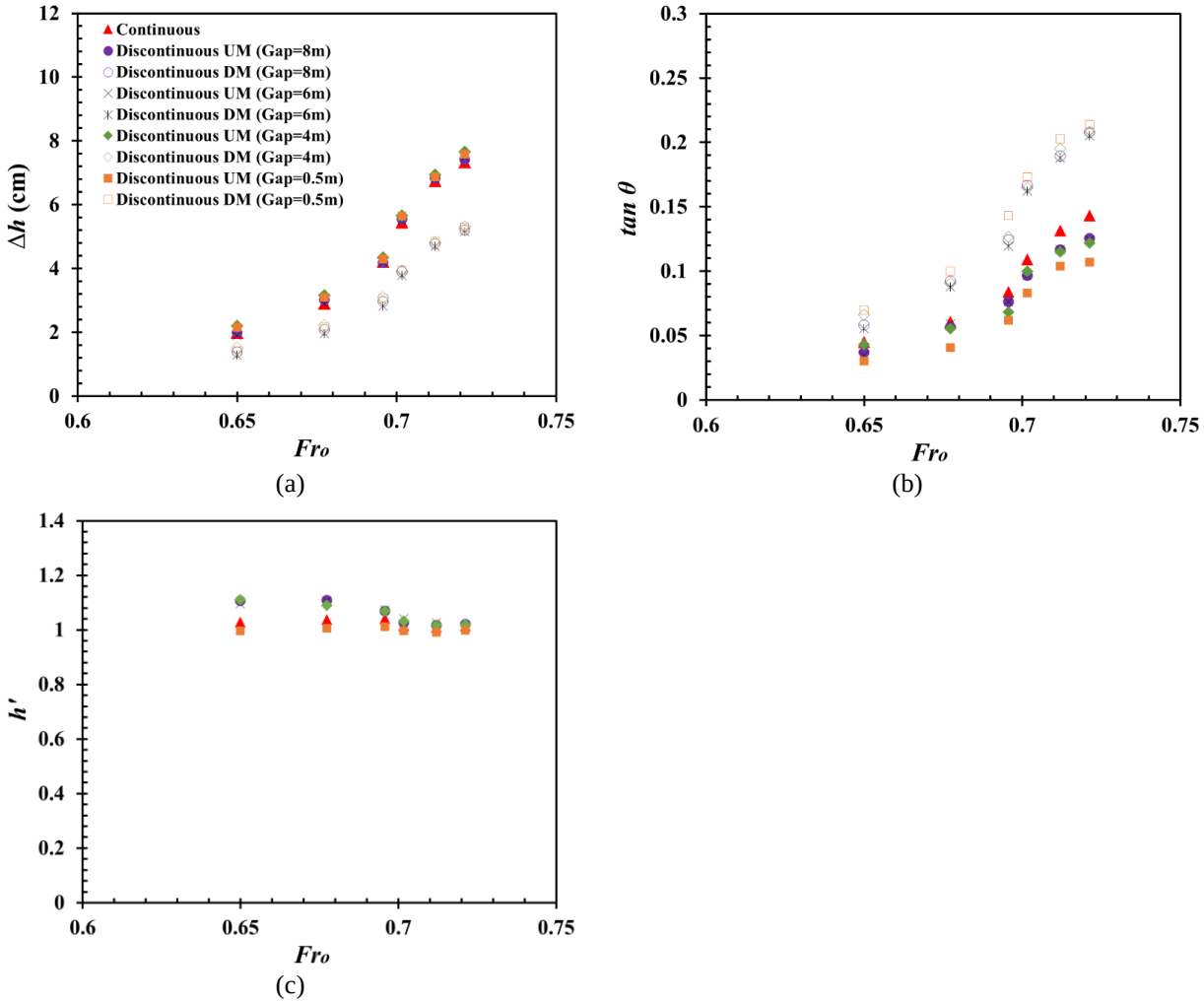

Figure 3: Flow structure analysis against varying Fr_o: (a) backwater rise (Δh) in the upstream of forest models, (b) water surface slope "$tan\,\theta$" within the forest models, and (c) inundation depth ($h'=h_i/h_o$) in the downstream of the forest.

3.2 Energy reduction

The water surface profiles (Figure 2) showed a significant difference between the effects of water depths in the upstream and downstream regions of forest models, which resulted in a certain loss of total flow energy. The energy loss ($\Delta E= (E_1-E_2)/E_1$, where E_1 is the mean specific energy at the forest front, whereas E_2 is the mean specific energy at the forest back) through the forest is the difference between the specific energy

upstream and downstream of the forest. The specific energy in the upstream and downstream of forest model is calculated in this study as $E = y + \alpha v^2/2g$ (Chow, 1959), where E is the specific energy, y is the flow depth, V is the velocity, and α is the velocity coefficient which is taken as 1.

Figure 4 shows the relative loss of flow energy through the forest models for all the considered configurations. A slightly increasing trend in energy loss is observed for all the cases with the increase in Fr_o condition. It can be observed that although the relative energy loss is slightly higher for CFM case only for the minimum considered Fr_o condition in comparison to those of DFM cases (except the case with Gap=0.5m); the energy loss became significantly higher, i.e. approximately 4-12%, for DFM cases (compared to that of CFM case) under the considered range of Fr_o. In general, the maximum loss of energy in DFM configuration is found to be 37%, whereas it was reduced to 32% in CFM configuration. Moreover, due to stronger reflection effect and relatively higher resistance to the flow in DFM case of minimum gap (Gap=0.5m), the energy reduction increased by a percentage difference of approximately 6-10% in comparison to those of other DFM cases, whereas it was further increased, i.e. approximately 10-15%, as compared to that of CFM case.

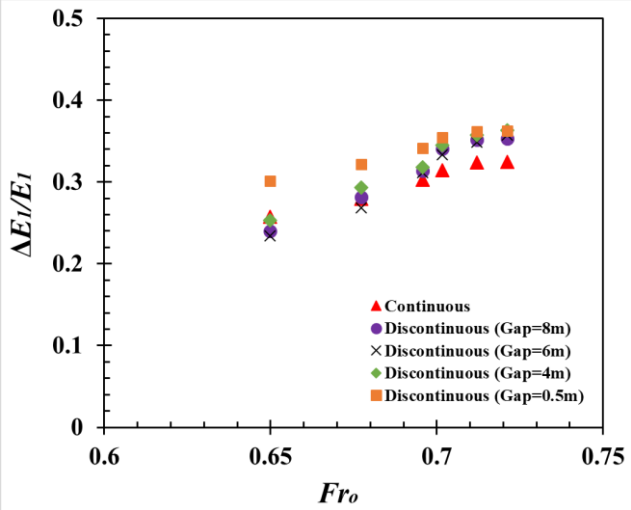

Figure 4: Relative total energy loss ($\Delta E_1/E_1$) for all the cases against varying Fr_o condition.

4. CONCLUSIONS

The present experimental study dealt with the investigation of flow structure analysis and energy reduction of tsunami current (approaching the inland region) through the coastal forest. The comparison of flow structures through a continuous and discontinuous forest, followed by a variety of gap distance between the forest models, is made under the subcritical flow conditions i.e. Fr_o= 0.650, 0.677, 0.696, 0.702, 0.712, and 0.721. The conclusions attained from this study are as follows:

- The propagating tsunami current experienced significant variations in the flow structures due to the resistance offered by the forest (either in CFM or DFM configurations), through which a noteworthy flow response has been captured. The drag due to the porous forest models narrowed the passage of fluid flow, and thus, resulted in a large difference in water levels between the upstream and downstream of forests, the intensity of which became stronger with the increase in Fr_o condition.

- With the same forest thickness, the backwater rise at the forest front became approximately 1-6% higher in DFM configurations as compared to that of CFM configuration. The stronger reflection effects in DFM cases (with all the considered gaps, i.e. 8, 6, 4, and 0.5m) created larger water surface slopes inside the DMs in DFM cases compared to that of CFM case. However, the downstream inundation depth was not significantly affected due to variation in forest configuration or gap length between the forest models.

- The difference in the specific energy at the forest front and the forest back resulted in a significant loss in the flow energy. The energy reduction was found to be approximately 4-12% higher in DFM cases (with a maximum loss of flow energy to be approximately 37%) as compared to that of CFM case (showing approximately 32% of maximum energy loss). Furthermore, the influence of minimum gap between the forest models, i.e. Gap= 0.5m, on the backwater rise, water surface slope, inundation depth, and ultimately on the energy loss was found to be comparatively more effective and noticeable.

The findings in this paper are important in providing knowledge about the effectiveness and comparison of thick (continuous) forest and discontinued forest (with the concept of the influence of the gap length between the forests) against tsunamis. The results showed that the discontinued forest with a minimum possible longitudinal gap between the forests could be a possible solution not only for a sufficient reduction of tsunami flow energy but also to the land-use limitation for the forest construction around the coastal regions. Therefore, we propose that the discontinuous (patch type) forest (as a double forest defense system) could be a better solution for designing an improved natural mitigation system against tsunamis. This could also be a feasible solution when the existing pathways are limited for the construction of a thick forest. As the primary objective of the natural defense system like coastal forest is to strengthen the resistance and increase the energy reduction, a further experimental study is required to investigate the influence of density parameter of the forest. These future studies should focus on its possible construction in the actual field as well for an effective mitigation strategy against tsunami flows and floods. Moreover, the reduction of its failing susceptibility against the approaching tsunamis must also be considered while designing an optimum solution.

REFERENCES

Anjum, N. and Tanaka, N. (2019). Experimental study on flow analysis and energy loss around discontinued vertically layered vegetation. *Environmental Fluid Mechanics*, doi:10.1007/s10652-019-09723-8

Chow, V.T. (1959). Open Channel Hydraulics. McGraw-Hill Publishing Co., New York.

Dengler, L. and Preuss, J. (2003). Mitigation lessons from the July 17, 1998 Papua New Guinea tsunami. *Pure and Applied Geophysics*, 160: 2001–2031.

Harada, K. and Imamura, F. (2005). Effects of coastal forest on tsunami hazard mitigation–a preliminary investigation. In: Satake, K. (Ed.), Tsunamis: case studies and recent development. *Advances in Natural and Technological Hazards Research*, 279–292.

HYDRA: Automatic flow control system for hydraulic experiments, version 2.2.0, Maruto Corporation Co., Ltd.

Igarashi, Y. and Tanaka, N. (2018). Effectiveness of a compound defense system of sea embankment and coastal forest against a tsunami. *Ocean Engineering*, 151: 246–256

Iimura, K. and Tanaka, N. (2012). Numerical simulation estimating the effects of tree density distribution in coastal forest on tsunami mitigation. *Ocean Engineering*, 54: 223–232.

Nandasena, N.A.K., Sasaki, Y. and Tanaka, N. (2012). Modeling field observations of the 2011 Great East Japan tsunami: efficiency of artificial and natural structures on tsunami mitigation. *Coastal Engineering*, 67: 1–13.

Pasha, G.A. and Tanaka, N. (2016). Effectiveness of finite length inland forest in trapping tsunami-borne wood debris. *Journal of Earthquake and Tsunami*, 10 (2): 1650008. https://doi.org/10.1142/S1793431116500081

Pasha, G.A. and Tanaka, N. (2017). Undular hydraulic jump formation and energy loss in a flow through emergent vegetation of varying thickness and density. *Ocean Engineering*, 141: 308–325.

Rashedunnabi, A.H.M. and Tanaka, N. (2019). Energy reduction of a tsunami current through a hybrid defense system comprising a sea embankment followed by a coastal forest. *Geosciences*, 9: 247.

Spiske, M., Weiss, R., Bahlburg, H., Roskosch, J. and Amijaya, H. (2010). The TsuSedMod inversion model applied to the deposits of the 2004 Sumatra and 2006 Java tsunami and implications for estimating flow parameters of palaeo-tsunami. *Sedimentary Geology*, 224: 29–37.

Suppasri, A., Mas, E., Charvet, I., Gunasekera, R., Imai, K., Fukutani, Y., Abe, Y. and Imamura, F. (2013). Building damage characteristics based on surveyed data and fragility curves of the 2011 Great East Japan tsunami. *Natural Hazards*, 66: 319–341.

Tanaka, N., Sasaki, Y., Mowjood, M.I.M. and Jinadasa, K.B.S.N. (2007). Coastal vegetation structures and their functions in tsunami protection: experience of the recent Indian Ocean tsunami. *Landscape and Ecological Engineering*, 3: 33–45.

Tanaka, N. (2012). Effectiveness and limitations of coastal forest in large tsunami: conditions of Japanese pine trees on coastal sand dunes in tsunami caused by Great East Japan Earthquake. *Journal of Japan Society of Civil Engineers*, Serial B1 *Hydraulic Engineering*, 68(4): II_7–II_15.

Tanaka, N. and Igarashi, Y. (2016). Multiple defense for tsunami inundation by two embankment system and prevention of oscillation by trees on embankment. In: *Proceedings of 20th Congress of IAHR APD Congress*, 28-31, Colombo, Sri Lanka, pp. 1–8.

Tanaka, N., Yagisawa, J. and Yasuda, S. (2013). Breaking pattern and critical breaking condition of Japanese pine trees on coastal sand dunes in huge tsunami caused by Great East Japan Earthquake. *Natural Hazards*, 65: 423–442.

Tanaka, N., Yasuda, S., Iimura, K. and Yagisawa, J. (2014). Combined effects of coastal forest and sea embankment on reducing the washout region of houses in the Great East Japan tsunami. *Journal of Hydro-environment Research*, 8: 270–280.

Tappin, D.R., Evans, H.M., Jordan, C.J., Richmond, B., Sugawara, D. and Goto, K. (2012). Coastal changes in the Sendai area from the impact of the 2011 Tohoku-oki tsunami: interpretations of time series satellite images, helicopter-borne video footage and field observations. *Sedimentary Geology*, 282: 151–174.

Usman, F., Murakami, K. and Kurniawan, E.B. (2014). Study on reducing tsunami inundation energy by the modification of topography based on local wisdom. *Procedia Environmental Sciences*, 20: 642–650.

Yang, Y., Irish, J. and Weiss, R. (2017). Impact of patchy vegetation on tsunami dynamics. *Journal of Waterway, Port, Coastal, and Ocean Engineering*, 143(4): 04017005. https://doi.org/10.1061/(ASCE)WW.1943-5460.0000380